ON-ORBIT INVESTIGATION OF TRANSIENT MICRODYNAMIC DISTURBANCES ON A DEPLOYED TRUSS STRUCTURE

Michel D. Ingham[*]
Massachusetts Institute of Technology
Department of Aeronautics and Astronautics
Cambridge, MA 02139

Marie B. Levine[†]
Jet Propulsion Laboratory
California Institute of Technology
4800 Oak Grove Dr., M.S. 157-316
Pasadena, CA 91109

1. Introduction

The second Interferometry Program Experiment (IPEX-2) is a space flight experiment investigating the microdynamic behavior of a representative deployed truss structure. This experiment serves as a technology demonstration for the planned space telescopes in NASA's Origins Program, including the Space Interferometry Mission (SIM). IPEX-2 was flown on the STS-85 Shuttle Mission in August 1997, as a secondary payload mounted on the free-flying DaimlerChrysler Aerospace/DARA satellite pallet, Astro-SPAS. Figure 1 shows a photograph of the Astro-SPAS with the IPEX-2 test article, on-orbit. The main objective of this experiment is to demonstrate and characterize the occurrence of impulsive microdynamic-level disturbances, as a result of changes in the internal stress distribution of a statically indeterminate structure with nonlinear frictional mechanisms. Secondary objectives of the IPEX-2 experiment are determination of the

---

[*] Graduate Research Assistant; Student Member AIAA

[†] Microdynamics Project Element Manager, Space Interferometry Mission; Member AIAA

dynamic properties of the flight test article on-orbit, and determination of the dynamic response and propagation attenuation of known mechanical disturbances. Some preliminary results from the flight experiment have been previously published[1,2]. This paper updates those results and presents a summary of the IPEX-2 modeling and data analysis work completed to date.

In this experiment, the type of microdynamic disturbance most likely to occur is *thermal creak*, or *thermal snap,* which is a result of quasi-static or dynamic slip across a discontinuous interface. Non-uniform thermal loading across a structure, or mismatch in the coefficients of thermal expansion (CTE) between different components changes the normal-to-shear load distribution across discontinuous interfaces such as hinges, latches and joints. This leads to changes in the stress distribution which result in microslip or gross dynamic motion (a.k.a., thermal snap). It should be noted that interface slips are not only thermally-induced phenomena. Temperature variations are just one of the ways that loads can be applied to a structure. Slips can also occur from mechanical load redistribution within a system, such as would happen during configuration changes (e.g., deployment, moving components). Investigations of microslip mechanisms and the phenomenon of thermal snap have been performed at the University of Colorado[3,4,5] and at MIT[6,7]. Thermal snap is a disturbance of particular concern to engineers designing spacecraft with tight dimensional stability requirements, such as SIM. Data from the Hubble Space Telescope revealed transient disturbances, which were attributed to thermally-induced snapping[8]. Recent work in the fields of microdynamic characterization and modeling of structures with nonlinear mechanisms is shedding light on the sources of

thermal creak in space structures. Warren and Peterson discovered that abrupt changes in structural shape at the microdynamic level occur as a result of dynamically-induced relaxation of strain energy stored by friction mechanisms within the structure[9]. Current work at the University of Colorado and NASA Langley Research Center is focusing on the design of microdynamically stable mechanisms, which would render structures less susceptible to creaking behavior[10,11].

2. Experiment Description

This section provides a brief description of the IPEX-2 flight experiment, including the structural test article, instrumentation and flight experiment profile. A description of the IPEX-2 hardware and experiment configuration can also be found in papers written by Levine[1,2].

The second Interferometry Program Experiment, IPEX-2, flew on shuttle mission STS-85, in August 1997. IPEX-2 was a secondary payload on the reusable science satellite Astro-SPAS (A/S). The Astro-SPAS is a spacecraft developed by DaimlerChrysler Aerospace, which is launched into Earth orbit by the Space Shuttle and deployed for a free flight period of approximately 10 days. During IPEX-2, a nine-bay joint-dominated pre-loaded truss was cantilevered off the side of the CRISTA-SPAS (Figure 1). The truss is made up of graphite composite longerons and battens, with stainless steel cables and fittings. A close-up view of one bay is shown in Figure 2. Roughly 300 lbf of pretension in the diagonal cables result in compressive preloads of approximately 400 lbf and 430 lbf in the longerons and battens, respectively. The end-to-end length of the boom is

approximately 92 inches. The geometric and material properties of the boom have been fully documented[12].

The truss design incorporates numerous joints and mechanisms, which represent possible creak sources. Furthermore, there is a significant mismatch in the coefficients of thermal expansion of the composite truss members and the steel diagonal cables. This mismatch, coupled with the statically indeterminate design of the boom and the changing thermal environment on-orbit, provide the strain energy storage mechanism required for thermal creak behavior.

The instrumentation used to perform the on-orbit dynamic and thermal characterization of the structure includes 24 micro-g accelerometers, 8 load cells, 48 temperature sensors, and 2 proof-mass actuators. Six of the accelerometers and six load cells were collocated inside the boom-to-spacecraft interface (I/F) struts to characterize the six interface degrees-of-freedom. Sixteen accelerometers were installed along the boom (Figure 3), including two that were collocated with the two shakers and load cells at the tip of the boom. The shakers were used to perform on-orbit modal tests to characterize the linearity and modal properties of the boom. The remaining two accelerometers were installed on the A/S so as to provide information on the source of any vibrations measured on the boom. Of the 48 temperature sensors, 24 were located inside the accelerometer casings for calibration purposes, and the remaining 24 were distributed along the boom as follows: 16 collocated on the corner fittings with the accelerometers to monitor the ambient temperature in the event of a thermal snap, 2 placed on either side of a longeron

truss member to investigate thermal gradients across the member, 2 placed on either side of a batten truss member, 3 placed on the pulley plate fittings, and 1 placed on a corner fitting near the base of the boom.

Close to 50 hours of on-orbit data was recorded at a 1 kHz sampling rate with 16-bit accuracy, representing approximately 10 gigabytes of storage space. The overall noise floor is estimated to be 20 μg RMS up to 500Hz, with 1 μg RMS below 10 Hz. During the first 45 hours, the response of the boom during normal A/S operation modes was recorded. The active disturbance sources include gyros, thrusters, and other payloads. This period also included over 25 day/night and night/day transitions. A preliminary assessment of this period has been reported by Levine[1].

The last 5 hours of the A/S flight were specifically dedicated to IPEX-2; all other payloads were turned off. During this IPEX-dedicated period, a total of 14 multi-shaker modal tests were performed to assess the on-orbit structural dynamic properties of the boom. Two experiments were also dedicated to evaluating the boom response to specific A/S mechanical disturbances: gyro response without thrusters (the "quiescent gyro experiment"), and thruster pulsing with and without the gyros in the background (the "thruster pulsing experiment"). Data from these experiments will be discussed briefly in this paper.

The most important IPEX-2 experiment corresponds to one 5-minute segment, during which even the A/S gyros and thrusters were shut down, and the boom experienced a

sudden night to day transition. The only active mechanism on board was the flight data recorder. This "quiescent period" provides the minimum disturbance state of the A/S, and is the period most likely to be quiet enough to measure thermally induced microdynamics in the boom. A typical time history of this period, measured on an accelerometer mounted transversely to the boom's longitudinal axis, is shown in Figure 5. A spectrogram of the time history is also included to illustrate the time-varying nature of the frequency content of the disturbances. As can be seen, the quiescent period flight data is rich in dynamic response: forty-five different types of events were identified. This period is the focus of most of the flight data analysis performed to date.

3. Modeling

Finite element (FE) models of the IPEX-2 structure in its ground and flight configurations were built, for use in the dynamic analysis and data visualization tasks. Thorough descriptions of the different models created are available in previously released documents[12,13], and thus only a brief summary of the most significant results from the most recent model is presented here.

Figure 4 depicts a finite element model of the boom, coupled with a model of the Astro-SPAS platform. Modal frequencies from this coupled model are tabulated in Table 1 (column labeled 'Nominal Model; 25 deg C; 0-g'). The nominal model is assumed to be unconstrained, in 0-g and room temperature conditions.

The effect of on-orbit temperature loads was investigated, by applying a –65 deg C temperature change to the nominal model. The modal frequencies listed in Table 1 show that the first bending modes of the boom are essentially unchanged by the temperature load. The fundamental torsion mode is softened, going from 29.68 Hz down to 28.21 Hz. Not surprisingly, the SPAS-dominated modes are unaffected by the change in boom preload induced by the temperature change, while the frequencies of the diagonal drum modes increase. The application of the temperature load results in modes in which torsion, bending and A/S deformations are more highly coupled.

It is important to note that changes in internal stress distribution will affect potential snap mechanisms: the greater the change in internal load from the nominal loading condition, the sooner the critical load for slip of the nonlinear frictional mechanisms will be reached. Such changes in internal stress can arise due to a number of different sources, such as thermal load on a statically indeterminate structure with CTE mismatch, or on-orbit operations-induced mechanical load redistribution.

In order to investigate the effect of model fidelity on the modes, several modeling details were added to the nominal model, to better represent the actual system flown (e.g. the cable tray and the ESP plate supporting the free end latch/plunger mechanism). The modal frequencies up to 100 Hz from this detailed coupled model are presented in the last column of Table 1, for 0-g and room temperature conditions. The first three flexible modes are essentially unchanged from the nominal model. However, the addition of the cable tray and ESP plate results in extra modes at 45.9, 47.2 and 58.8 Hz, which were not

found in the nominal model. For both the nominal and detailed models, the global boom modes found in the 60 to 98 Hz range are coupled with local "drumming" of the pulley fittings on the diagonal cables, and also sometimes with SPAS deformations. The mode shapes and frequencies in this range are more significantly affected than the fundamental bending and torsion modes, due to the addition of the above-mentioned modeling details.

4. Summary of IPEX-2 Flight Data Analysis

Analysis of the quiescent period, the gyro period and the thruster pulsing sequences has yielded numerous interesting findings. In this section, these findings are summarized.

A catalog of the various disturbances seen during the quiescent period has been compiled[14], which reveals a wide variety in the types of events recorded. These events include steady-state disturbances, transient disturbances, and disturbances with time-varying frequency content. Figure 6 presents time history data from five different sensors, corresponding to the first 150 seconds of the 5-minute quiescent period. It is evident from these time traces that the nature and amplitude of the response to each event varies quite significantly across the structure. The microdynamic events are seen most frequently right after the night-to-day transition, which occurs between 30 and 70 seconds after the start of the quiescent period. Later in the quiescent period, less microdynamic activity is observed. This paper provides detailed characterizations of a representative selection of events. A complete overview of the analysis results from the quiescent period data can be found in other documents[14,15].

The occurrence of impulsive microdynamic-level disturbances has been demonstrated on-orbit. The analysis to date suggests that some of these events were thermally-induced structural disturbances. IPEX-2 represents the first known, deliberate attempt to characterize such disturbances on-orbit, though on-orbit operational data from the Hubble Space Telescope has shown evidence of impulsive thermally-induced structural phenomena[8], and a demonstration of thermal creak observed in a ground laboratory environment has been previously documented[6].

A preliminary localization of the source of the impulsive events was attempted, based on observed delays in the time of occurrence of the events at different sensor locations across the structure. Some of the events apparently originated either on the Astro-SPAS or at the SPAS/boom interface, while others appear to have originated on the IPEX boom.

A quantitative characterization of the identified disturbances was performed:

- The quiescent period thruster pulses induce RMS response on the boom of 300 μg in acceleration, 2 μm/s in velocity and 5 nm in displacement (see Figure 7). The worst-case firing direction in the thruster pulsing sequence following the quiescent period resulted in RMS response amplitudes on the order of 1.5 mg, 5 μm/s and 15 nm (see Figure 8).
- During the quiescent gyro experiment, the response to the gyros was felt at 200 Hz and 495 Hz (aliased down from 800 Hz and 505 Hz, respectively). The broadband RMS of the boom response to the gyros is about 50 μg to 80 μg in the lateral

directions, and 120 μg in the axial direction. Figure 9 shows a time trace and spectrogram from the gyro experiment.

- One type of impulsive disturbance, associated with the flight data recorder, was found to occur every 14.4 seconds. The response to these disturbances was felt most significantly on the boom accelerometers, reaching peak acceleration, velocity and displacement levels of 300 μg, 5 μm/s and 15 nm, respectively (see Figure 10).
- Narrowband 43 Hz disturbances were seen in the data, building up and decaying over a period of 5 seconds or so. Such events occurred twice in the quiescent period experiment, and at least once in the quiescent gyro experiment. Peak amplitudes of over 400 μg, 15 μm/s and 50 nm were seen in response to these narrowband disturbances (see Figure 11).
- Finally, numerous broadband, impulsive events were identified as possible thermal creaks. The response levels seen for these disturbances vary widely, but in general, peak accelerations in the range from 300 μg to 700 μg were recorded. Peak integrated velocities were generally on the order of 5 μm/s, and the peak integrated displacements were generally less than 50 nm. These integrated velocities and displacements were often dominated by low-frequency noise, but at least one event (suspected to have had its source on the A/S or at the SPAS/boom interface) introduced peak velocities and displacements on the order of 40 μm/s and 3 microns, respectively. Figures 12 and 13 show representative impulsive events, with assumed SPAS source and boom source, respectively.

The existence of such impulsive microdynamic phenomena suggests that precision optical spacecraft requirements expressed in terms of RMS quantities may be inadequate. Short transient disturbances, which are insignificant in a time-averaged, RMS sense, may nonetheless be unacceptable if they cause a telescope's optics to lose their metrology lock, for example. Requirements expressed in terms of peak perturbation levels and rates should be considered.

References

[1] Levine, M.B., "The Interferometry Program Flight Experiments: IPEX I & II", Proc. SPIE Astronomical Telescopes and Instrumentation Conference, Kona, HI, March 1998, Paper 3350-14.

[2] Levine, M.B., "Microdynamic Behavior of a Joint Dominated Structure On-orbit", 40th SDM Conference, St. Louis, MO, April 12-15, 1999, AIAA paper #99-1267.

[3] Hinkle, J.D. and Peterson, L.D., "An Experimental Investigation of Roughness-Induced Microslip in Metallic Interfaces", 40th SDM Conference, St. Louis, MO, April 12-15, 1999, AIAA paper #99-1382.

[4] Hachkowski, M.R., Peterson, L.D. and Lake, M.S., "Analytical Model of Nonlinear Hysteresis Mechanisms in a Rolling Element Joint", 40th SDM Conference, St. Louis, MO, April 12-15, 1999, AIAA paper #99-1268.

[5] Hardaway, L.M.R. and Peterson, L.D., "Microdynamics of a Precision Deployable Optical Truss", Proceedings of the SPIE Annual Meeting, Denver, Colorado, July 1999, SPIE paper #3785-01.

[6] Ingham, M., Kim, Y., Crawley, E., McManus, H., and Miller, D.,"Experimental Characterization of Thermal Creak Response of Deployable Space Structures", 40th SDM Conference, St. Louis, MO, April 12-15, 1999, AIAA paper #99-1269.

[7] Kim, Y.A., McManus, H.L., and Miller D.W., "Thermal Creak Induced Dynamics of Space Structures", Ph.D. Thesis, Dept. of Aeronautics and Astronautics, MIT, Cambridge, MA, February 1999, SERC Report #14-98.

[8] Blair, M., and Sills, J., "Hubble Space Telescope On-Orbit System Identification", Proc. 12th International Modal Analysis Conference, Honolulu, HA, February 1994, pp. 663-669.

[9] Warren, P.A., and Peterson, L.D., "Sub-micron mechanical stability of a prototype deployable space structure", 38th SDM Conference, Kissimmee, FL, April 7-10, 1997, AIAA paper #97-1375.

[10] Hinkle, J.D., Warren, P.A., and Peterson, L.D., "Design and Testing of an Optical Precision Deployment Latch", 40th SDM Conference, St. Louis, Missouri, April 12-15, 1999, AIAA paper #99-1270.

[11] Lake, M.S., Fung, J., Gloss, and K., Liechty, D.S., "Experimental characterization of hysteresis in a revolute joint for precision deployable structures", 38th SDM Conference, April 7-10, 1997, AIAA paper #97-1379.

[12] Ingham, M., and Levine, M., *IPEX-2 Flight Configuration Modeling Task Report*, Jet Propulsion Laboratory Document JPL D-16986, March 16, 1999.

[13] Peng, C.-Y., Levine-West, M., and Tsuha, W., *Interferometry Program Experiment IPEX-II Pre-flight Ground Modal Test and Model Correlation Report*, Jet Propulsion Laboratory Document JPL D-14809, September 19, 1997.

[14] Ingham, M., and Levine, M., *IPEX-2 Quiescent Period On-Orbit Event Catalog*, Jet Propulsion Laboratory Document JPL D-17821, May 15, 1999.

[15] Ingham, M., and Levine, M., *IPEX-2 Flight Data Analysis: Quiescent Period Report*, Jet Propulsion Laboratory Document (to be published).

Figure 1. Astro-SPAS and IPEX-2 on-orbit

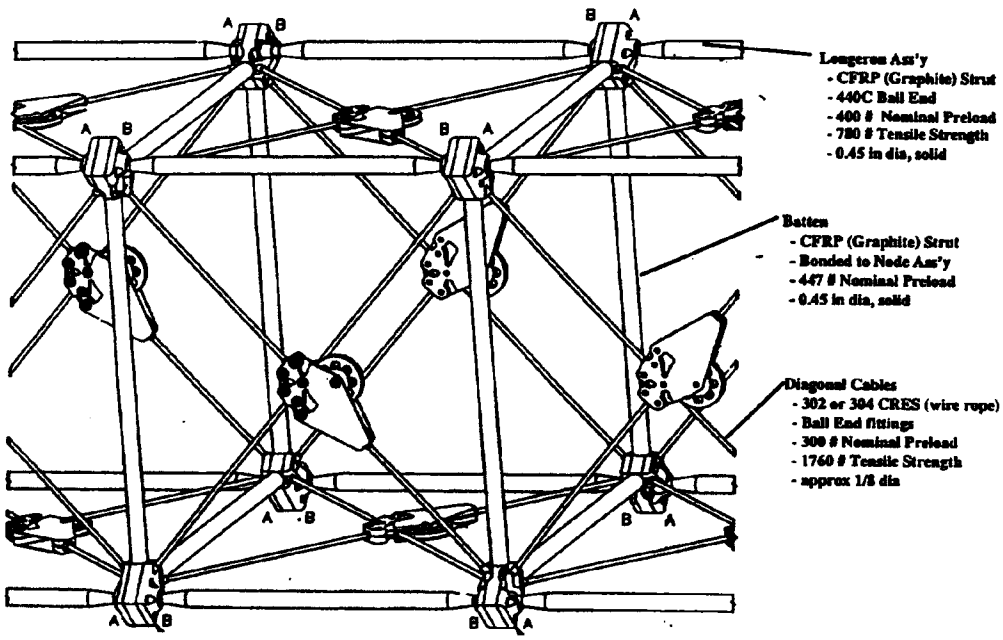

Figure 2. Close-up view of single bay

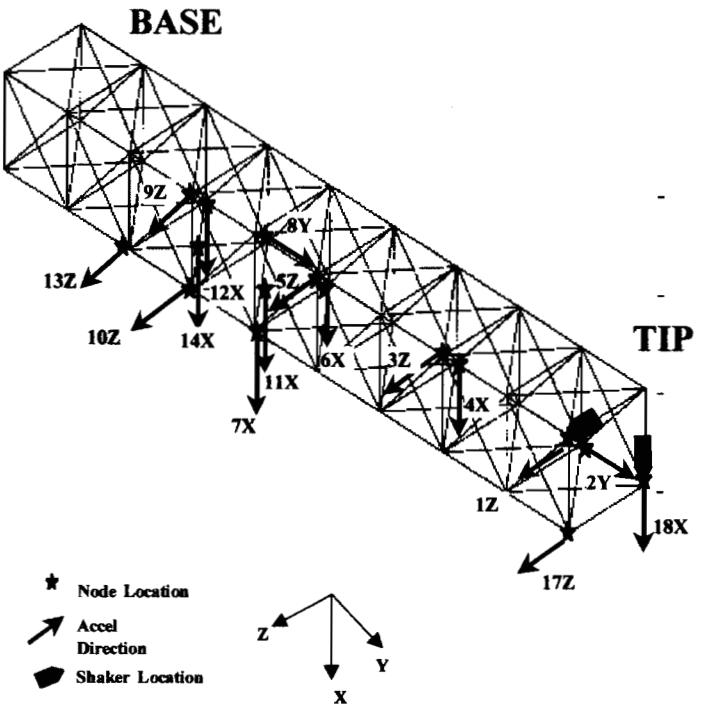

Figure 3. Boom-mounted accelerometer locations

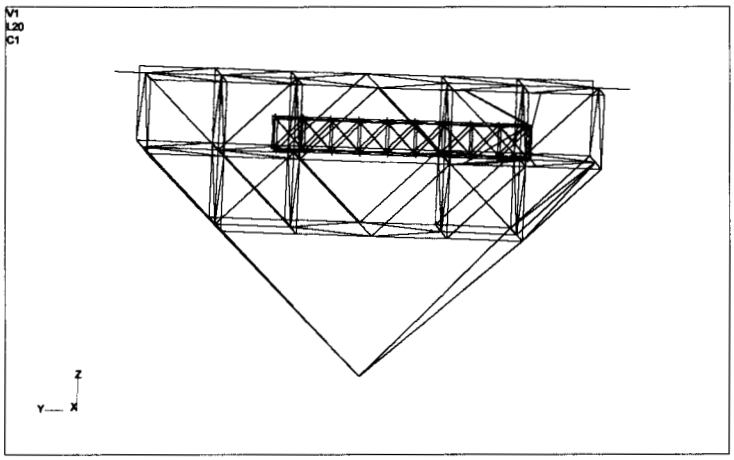

Figure 4. Coupled SPAS/boom model

Table 1. Flexible modes of the coupled model (up to 100 Hz)

Description B: boom bending; T: boom torsion	Nominal Model 25 deg C; 0-g	Nominal Model -40 deg C; 0-g	Detailed Model 25 deg C; 0-g
B1	12.53	12.53	12.53
B1	18.37	18.37	18.37
T1	29.68	28.21	29.68
SPAS-dominated modes (some coupled with B & T)	34.81 39.81 41.18 48.47	34.81 39.81 41.18 48.47	35.33 39.56 41.15 45.91 (tray) 47.22 (tray) 48.45
Diagonal drum modes (accels A11 & A14)	54.64 54.85 56.61	54.80 60.01 60.89 61.60 65.41	54.66 54.98 56.61
SPAS & ESP plate mode	-	-	58.83
Diagonal drum modes (some coupled with B & T, and SPAS deformation)	60.04 up to 97.68	66.29 up to 97.63	61.30 up to 98.08

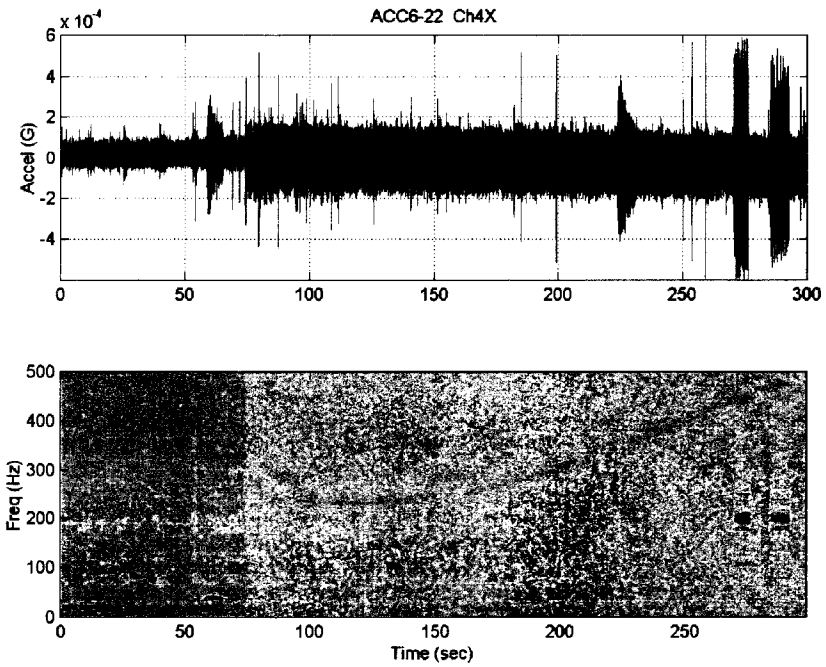

Figure 5. Time history and spectrogram for the quiescent period, obtained at accelerometer A4

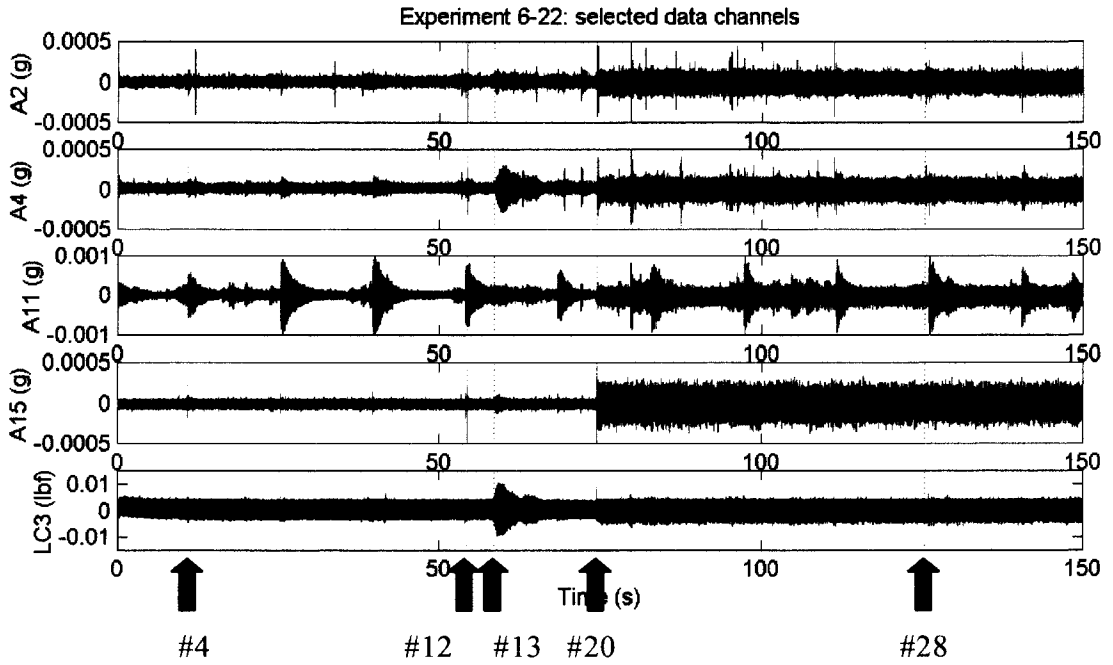

Figure 6. Quiescent period time histories from various sensors (arrows indicate selected events seen in the data, numbered according to the event catalog[14])

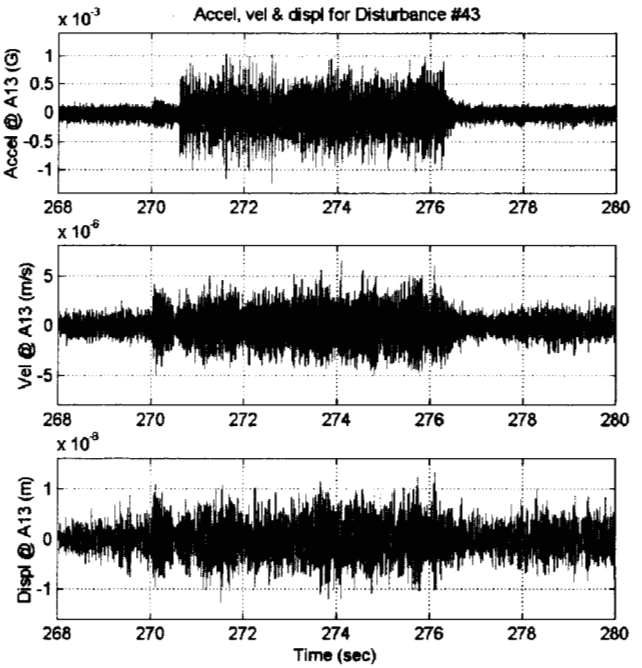

Figure 7. Acceleration, velocity & displacement for thruster disturbance (accelerometer A13)

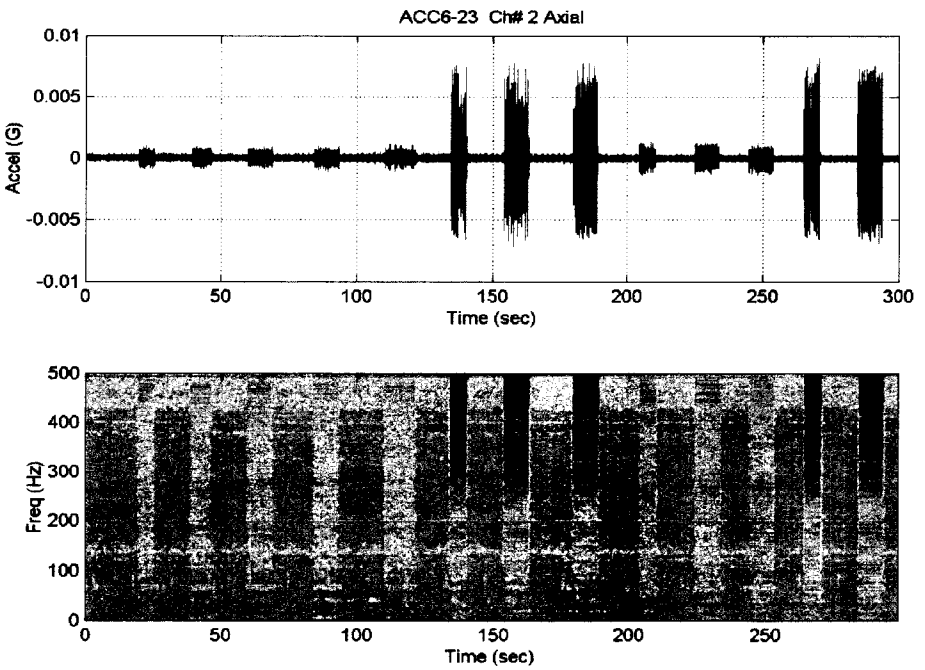

Figure 8. Time history and spectrogram from the dedicated thruster pulsing experiment, recorded at accelerometer A2

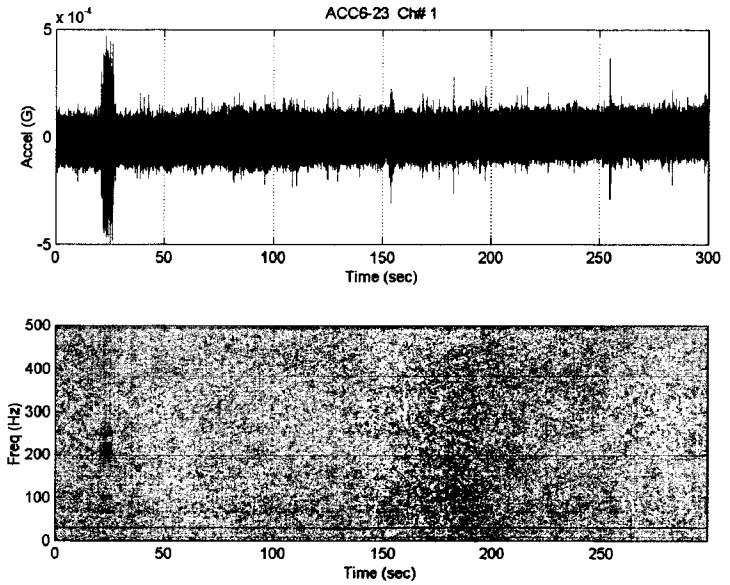

Figure 9. Time history and spectrogram from the quiescent gyro period (accelerometer A1)

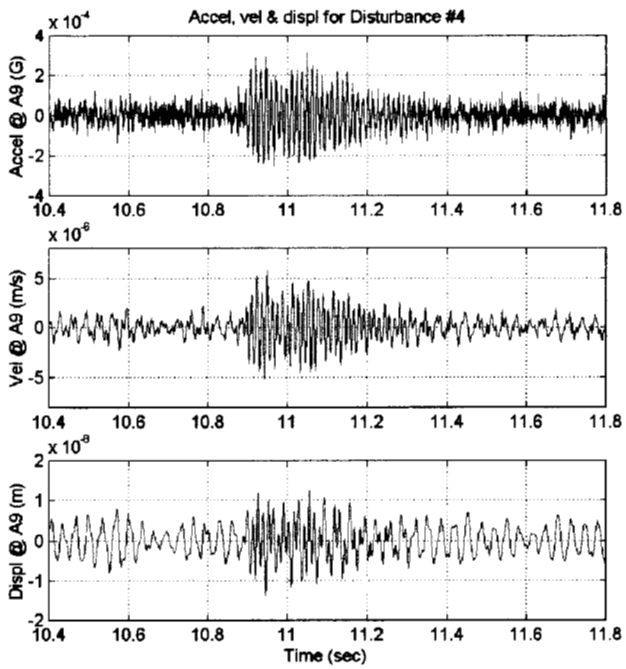

Figure 10. Acceleration, velocity & displacement for tape recorder Disturbance #4 (accelerometer A9)

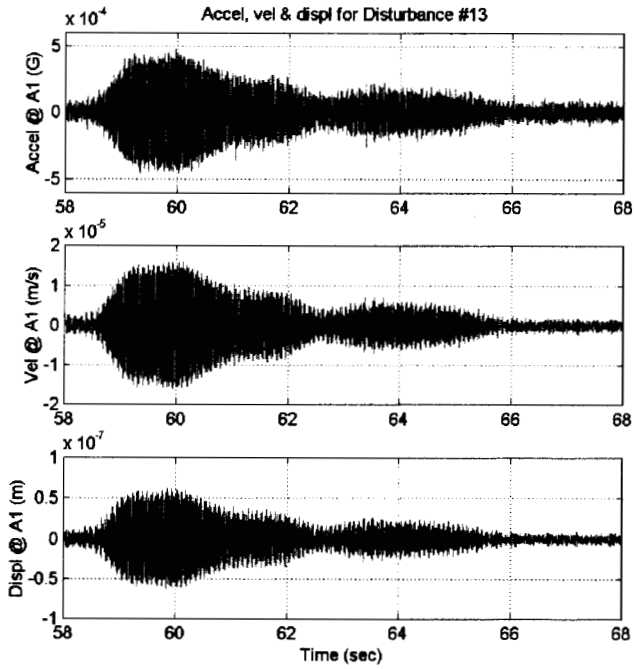

Figure 11. Acceleration, velocity & displacement for narrowband Disturbance #13 (accelerometer A1)

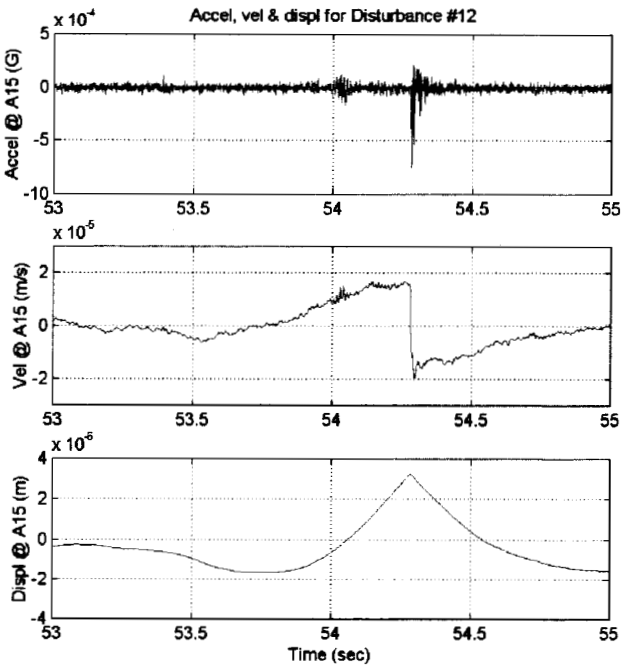

Figure 12. Acceleration, velocity & displacement for impulsive Disturbance #12, with assumed A/S source (SPAS accelerometer A15)

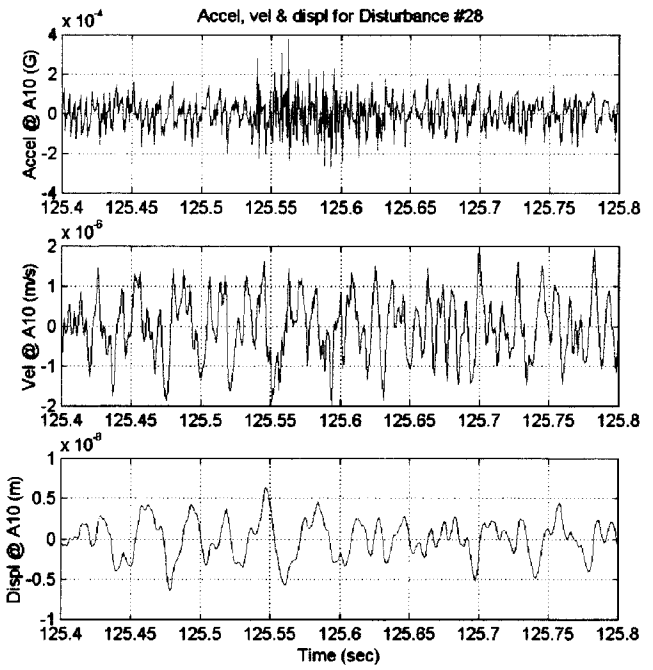

Figure 13. Acceleration, velocity & displacement for impulsive Disturbance #28, with assumed boom source (accelerometer A10)